



Contents lists available at ScienceDirect



# Catalysis Today

journal homepage: [www.elsevier.com/locate/cattod](http://www.elsevier.com/locate/cattod)

## In situ XANES study of Cobalt in Co-Ce-Al catalyst applied to Steam Reforming of Ethanol reaction

Arthur E.Pastore de Lima <sup>a,b</sup>, Daniela C. de Oliveira <sup>a,\*</sup>

<sup>a</sup> Brazilian Synchrotron Light Laboratory, LNLS, Caixa Postal 6192, CEP 13083-970 Campinas, SP, Brazil

<sup>b</sup> Universidade Estadual de Campinas, UNICAMP, Campinas, SP, Brazil

### ARTICLE INFO

#### Article history:

Received 24 September 2015

Received in revised form 20 January 2016

Accepted 25 February 2016

Available online xxx

#### Keywords:

Hydrogen

Ethanol

Ceria

Catalyst

Cobalt

XANES

### ABSTRACT

The effect of ceria in cobalt-ceria-alumina catalyst was studied using *in situ* X-ray near edge spectroscopy (XANES) at Co K-edge and Ce L<sub>III</sub>-edge. The introduction of ceria in this catalyst resulted in a significant removal of Co from CoAl<sub>2</sub>O<sub>4</sub> spinel phase to Co and CoO phases. The Co K-edge revealed the symmetry changes in Co according to the temperature and atmosphere in reduction process. We also showed the stability of Co sites as well the oxidation state of ceria in operando steam reforming of ethanol (SRE) reaction. After reduction of Ce<sup>4+</sup> to Ce<sup>3+</sup>, no significant changes were observed by XANES. Gas Chromatography (GC) analysis showed a high ethanol conversion at 500 °C, high hydrogen yield and low formation of undesired products as methane and ethylene. The results showed a Co/Ce/Al<sub>2</sub>O<sub>3</sub> catalyst as promising material to be applied in hydrogen production in SRE reaction.

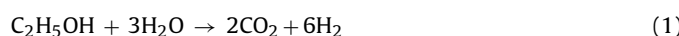
© 2016 Elsevier B.V. All rights reserved.

### 1. Introduction

The growing need of a more rational use of natural resources has drawn high interest in hydrogen (H<sub>2</sub>) production, especially from renewable sources [1]. The use of H<sub>2</sub> on fuel cells in automobiles involves the production of this gas at the time of use, to avoid problems related to its storage and transportation.

The hydrogen production from methanol and hydrocarbons is widely studied in reforming reactions; however, the reforming of these compounds releases CO<sub>2</sub>, which is harmful to the environment [2,3]. But hydrogen can also be obtained from bio-ethanol, for example, in a sustainable and clean way [4], through the Steam Reforming of Ethanol (SRE), a very simple catalytic process. This reaction also releases CO<sub>2</sub>, but the crops that produce bio-ethanol (for SRE), such as sugarcane and corn, require CO<sub>2</sub> to grow and develop, balancing the emission of this gas [2,3,5].

Steam Reforming of Ethanol consists in reacting ethanol and water, at moderate temperatures, to produce CO<sub>2</sub> and H<sub>2</sub>. Literature reports different mechanisms for SRE, under the influence of different catalysts supported in different materials [2–10]. The general reaction is represented in Eq. (1) [5].



The reaction pathway follows through dehydrogenation of ethanol, acetaldehyde steam reforming reaction and water-gas shift reaction (WGSR). Parallel reactions may occur in Steam Reforming of Ethanol reaction. Decomposition of ethanol produces methane, carbon monoxide and hydrogen; and the dehydration of ethanol produces ethylene, which can lead to coke formation on catalyst surface, causing its deactivation [11].

SRE has been widely studied and a large variety of materials can be used under soft reaction conditions. The great interest on the development of new active catalysts has contributed to understand the mechanisms, to enhance the hydrogen selectivity while the coke formation over the material can be minimized [4].

Choosing the catalysts is essential to SRE, because they may improve the selectivity to desired product and minimize the parallel reactions. Ideally, catalyst must maximize ethanol conversion and hydrogen selectivity, convert the CO produced to CO<sub>2</sub> and avoid coke formation over catalyst surface. Many transition metals have been studied as catalyst active phase as Ni, Co, Cu, Fe [12]. For this purpose, the non-noble metals Ni and Co have showed efficient catalytic activity for SRE reaction [5]. The interest in cobalt catalyst has been reinforced thanks to their activity to break C–C bonds [13], and their low cost, high activity and selectivity to hydrogen [12]. It is then noteworthy that many authors [12–14] have demonstrated that cobalt is an alternative to nickel due to the effectiveness of this catalyst in the SRE.

\* Corresponding author.

E-mail address: [doliveira@lnls.br](mailto:doliveira@lnls.br) (D.C. de Oliveira).

Many different supports can be used in SRE, which can play an active role in the reaction depending on composition, morphology and particle sizes. In particular, ceria has been widely studied as active support in SRE with reports showing that different particles sizes have significant activity, especially at high temperatures. However, the C–C bond cleavage activity was seen to be low [15–17]. Also, Song and Ozkan [18] reported on the positive effect of ceria to avoid deactivation by coke, due to the high oxygen mobility in ceria oxide, which improves the catalytic stability. All these interesting properties have highlighted the outstanding catalytic properties of Co/ceria system in SRE [19].

Several techniques have been used to characterize inorganic solids in order to obtain morphological, structural and/or textural information of catalysts [20]. Among other techniques, XAS (X-Ray Absorption Spectroscopy) in the near edge region XANES (X-Ray Absorption Near Edge Structure) provides information of the oxidation state of absorber atom, the spatial arrangement of neighborhood and the density of unoccupied states [21,22]. Moreover, the high penetration of hard X-rays allows to investigate catalysts under *operando* conditions [23].

With all that in mind, the goal of this work was to study the structure of Co-supported on ceria-alumina catalysts by XANES during activation under H<sub>2</sub> and in SRE reaction. We also aimed at studying the catalytic activity for Steam Reforming of Ethanol reaction, seeking for the optimal conditions to achieve high ethanol conversion, hydrogen selectivity and catalyst stability. We show that the presence of ceria affects the catalyst structure allowing hydrogen production in our catalytic tests under SRE conditions.

## 2. Experimental

### 2.1. Catalyst preparation

The catalyst was prepared by the wet impregnation method. An aqueous solution of CoCl<sub>2</sub>·6H<sub>2</sub>O and Ce(NO<sub>3</sub>)<sub>3</sub>·6H<sub>2</sub>O was added to Al<sub>2</sub>O<sub>3</sub> (all Sigma-Aldrich reagents). The mixture was stirred over 1 h and then dried overnight at 100 °C. The solid obtained was calcined at 800 °C over 8 h in air to remove residual components. We defined the initial concentrations to obtain a final solid with molar composition of 5% of CoO, 10% of Ce<sub>2</sub>O<sub>3</sub> and 85% of Al<sub>2</sub>O<sub>3</sub>. The sample was named Co5Ce10Al.

### 2.2. Catalytic reaction

Preliminary catalytic tests were performed to find the experimental conditions of activation and reaction using a mass spectrometer (MS). To assess the catalytic activity of the Co5Ce10Al sample, a gas chromatograph (GC-Agilent) equipped with a FID (flame ionization detector) and a TCD (thermal conductivity detector) was used. The reaction was carried out in a quartz tube reactor with 12 mm of diameter. First we activated the sample at 800 °C for 1 h under continuous flow of diluted hydrogen (100 mL/min, 5% H<sub>2</sub>/He). Then we cooled down the furnace temperature to 200 °C and the reaction mixture was fed into the reactor. Catalytic tests were carried out from 200 °C to 700 °C. We used a ratio of 3:1 of H<sub>2</sub>O:ethanol (steam); a total flux of 100 mL/min of He was used to feed the reactants into the reactor. We analyzed the products of reaction each 100 °C over 1 h (5 injections per temperature). The quantification (Table 1) was obtained by comparing the area under the corresponding GC peak with the calibration performed preliminary with each component of the reaction products and reactants. Ethanol conversion, hydrogen yield and products selectivity were calculated with the following equations [24,25].

$$\chi_{EtOH} = \frac{n_{in,EtOH} - n_{out,EtOH}}{n_{in,EtOH}} \quad (2)$$

$$R_{H_2} = \frac{n_{H_2}}{6 \times (n_{in,EtOH} - n_{out,EtOH})} \quad (3)$$

$$S(j) = \frac{n_j \times \psi_j}{\sum_i [n_i \times \psi_i]} \quad (4)$$

$$S(H_2) = \frac{n_{H_2} \times \xi_{H_2}}{\sum_i [n_i \times \xi_i]} \quad (5)$$

where  $\chi_{EtOH}$  is the ethanol conversion;  $n_j$  is the amount of substance of component  $j$ ;  $R_{H_2}$  is the hydrogen yield;  $S(j)$  is the selectivity for component  $j$ ;  $\psi_j$  is the number of carbon atoms present in molecule  $j$ ; and  $\xi_j$  is the number of hydrogen atoms present in molecule  $j$ . The index  $i$  represent only the reaction products.

### 2.3. Catalyst characterization by XANES

XANES *in situ* experiments were done at the Brazilian Synchrotron Light Laboratory (LNLS) on D04B (XAFS1) beamline. XAS spectra were recorded at the cobalt K-edge (E = 7709 eV) and cerium L<sub>III</sub>-edge (E = 5723 eV) using a channel-cut Si(111) monochromator. The harmonic contamination at the XAFS1 beamline is less than 0.1% above ~4300 eV.

The data collection was carried out in transmission mode using ion chamber detectors to measure the incident (I<sub>0</sub>) and transmitted (I<sub>1</sub>) x-rays intensities. The reference samples used in this study were obtained from commercial sources with 99.99% purity. To acquire the spectrum we used 0.5 and 0.3 eV energy step at XANES region of Ce L<sub>III</sub>-edge and Co K-edge around the edge, respectively, counting 1 s/point. The total time to measure each spectrum was about 20 min at Ce L<sub>III</sub>-edge and 10 min at Co K-edge. The Co5Ce10Al catalyst was studied by XANES along the *in situ* activation process (reduction of Co oxide) and in SRE *operando* conditions. The required amount of samples were mixed with boron nitride to achieve the optimal sample thickness with a jump of  $\Delta\mu = 0.58$  and  $\Delta\mu = 0.14$  for Ce L<sub>III</sub>-edge and Co K-edges measurements, respectively. Cobalt and chromium metal foils were used as a reference for energy calibration. An *in situ* cell was used in order to carry out the x-ray absorption measurement at realistic SRE reaction conditions. The cell consists of a quartz tube in a ceramic furnace heated by a Cr-Al thread. The quartz tube is sealed by a Kapton window supported in a connector with standard Swagelok 1/4" where unions fixed at both extremity of the tube permit a gas flux through the sample pellet. Gas flow was supplied by a mobile gas distribution set controlled by commercial flow meters. The temperature programmed reduction was carried out by heating the pellet up to 800 °C under 100 mL/min flow of 5% H<sub>2</sub>/He, keeping the temperature constant by 1 h before stopping heating and then cooling the sample to the ambient temperature under He flow. Following, the sample was heated to 400 °C and we introduced the ethanol and water to start the SRE; then the reaction was also performed at 500 °C. All this process was followed by XANES spectra every ~10 min and mass spectrometry (MS) to check the SRE reactants and products.

## 3. Results and discussion

### 3.1. Catalyst characterization

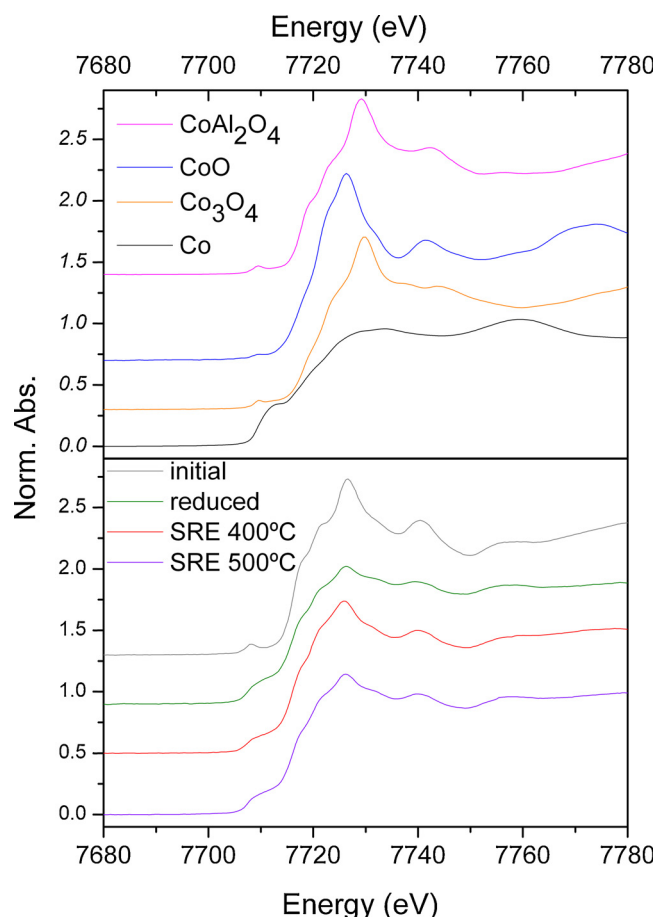
#### 3.1.1. XANES study at Co K-edge

From XANES data at Co K-edge the information about geometry and oxidation state can be attributed by qualitative analysis. Fig. 1 shows the XANES of Co K-edge of some cobalt compounds. The Co from Co5Ce10Al sample is in CoAl<sub>2</sub>O<sub>4</sub> structure, which has spinel geometry where the cobalt ions (Co<sup>2+</sup>) occupy only tetrahedral (Td) sites while the aluminum ions are in the octahedral (Oh) sites. The other common compound with spinel structure is Co<sub>3</sub>O<sub>4</sub> with two

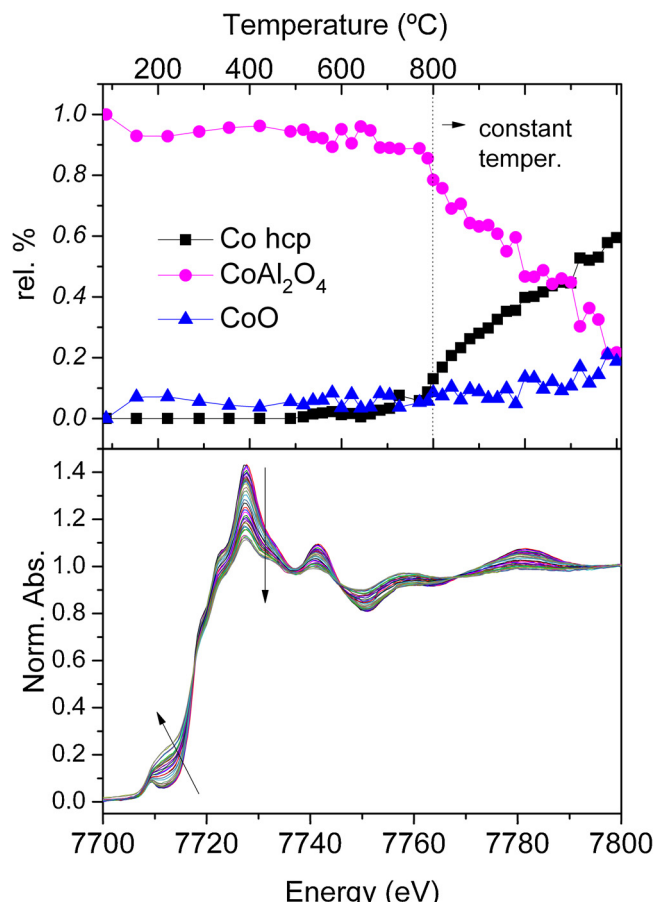
**Table 1**

Ethanol conversion, hydrogen yield and selectivity to the SRE products to the Co5Ce10Al catalyst.

Co5Ce10Al	400 °C	500 °C	600 °C	700 °C
Ethanol conversion	(22.1 ± 0.7)%	(84 ± 2)%	(100 ± 0)%	(100 ± 0)%
H <sub>2</sub> yield	(51.4 ± 0.8)%	(51.8 ± 0.4)%	(64.3 ± 0.2)%	(62.0 ± 0.3)%
S(H <sub>2</sub> )	(67.4 ± 0.8)%	(77.7 ± 0.5)%	(97.6 ± 0.03)%	(95.4 ± 0.1)%
S(CO <sub>2</sub> )	(15.6 ± 0.5)%	(41.0 ± 1)%	(59.0 ± 2)%	(59.0 ± 1)%
S(CH <sub>4</sub> )	(3.0 ± 1)%	(2.2 ± 0.3)%	(2.4 ± 0.03)%	(4.51 ± 0.09)%
S(Acetaldehyde)	(61.7 ± 0.7)%	(20.0 ± 2)%	-	-
S(CO)	(13.0 ± 2)%	(16.1 ± 0.8)%	(38.0 ± 2)%	(36.2 ± 0.9)%
S(Acetic acid)	-	-	-	-
S(Ethylene)	-	(4.7 ± 0.2)%	-	-
S(Acetone)	(6.1 ± 0.4)%	(15.0 ± 2)%	-	-

**Fig. 1.** (top) XANES at Co K-edge from reference compounds; from top to bottom: CoAl<sub>2</sub>O<sub>4</sub>, CoO, Co<sub>3</sub>O<sub>4</sub> and Co metal; (bottom) XANES at Co K-edge from Co5Ce10Al sample under different conditions along the activation and SRE reaction.

thirds of the cobalt ions occupying Oh sites with oxidation state 3+ and a third of the cobalt ions occupying Td sites with oxidation state 2+. But to the later compound the intensity of the pre-edge peak, which is attributed to the 1s–3d transition, is lower. The pre-edge intensity is related to the occupancy as well the symmetry of the 3d shell. In the case of Td coordination, the dipole-forbidden 1s–3d transition becomes partially dipole-allowed by the asymmetry and it results in a pre-edge peak. With Oh coordination, the pre-edge peak is less intense or absent, only appearing if the center of symmetry is broken, allowing the 1s–3d transition. Another reference sample such as CoO has only Oh sites for Co, and therefore the pre-edge feature is very weak. In Co5Ce10Al initial sample, a well defined pre-edge peak can be observed around 7709 eV. Other important feature observed in the initial sample is the strong edge

**Fig. 2.** (top) Relative Co compounds fractions in the Co5Ce10Al sample as a function of reduction temperature extracted from the XANES at Co K-edge reported in the bottom part; (bottom) evolution of the Co K-edge XANES of Co5Ce10Al sample along the reduction process.

shoulder, characteristic of the higher occupancy of Co<sup>2+</sup> in Td sites as CoAl<sub>2</sub>O<sub>4</sub> [26].

XANES measurements in Temperature Programmed Reduction (TPR) were used to obtain information about phase changes of Co as a function of the temperature under hydrogen atmosphere showed in Fig. 2. The first changes in the spectra were observed at low temperatures up to ~490 °C, where the white line starts to decrease (the main absorption peak owing to 1s–4p transition, with area under the peak directly related to the number of unoccupied states in the 4p), which can be attributed to the water removal from the sample. There is no energy shift along the reduction up to ~700 °C and the pre-edge as well as the white line remain unchanged. From ~700 °C to 800 °C the decrease in the intensity of white line is evident. After that temperature, the increase in the pre-edge is concomitant to

the white line decrease with the reduction process carrying on at constant temperature of 800 °C.

XANES Co K-edge measurements were also performed during SRE tests, also showed in Fig. 1. At 400 °C, just before start the SRE, the sample spectrum has basically the same features of the final reduced sample, with a very small increase in the white line intensity attributed to some oxidation and/or temperature effect. When we start SRE reaction at 400 °C, we observe that the water and ethanol presence doesn't affect significantly the Co local geometry except for another small amount of oxidation that tends to disappear along the time. When the temperature is increased to 500 °C, the white line intensity decrease, which indicate a cobalt reduction due to the temperature and/or products from reaction.

The relative composition of sample presented in Fig. 2 (top) was obtained by linear combination fitting of standards spectra. The initial sample was obtained ~97% of  $\text{CoAl}_2\text{O}_4$ . At the end of reduction at 800 °C, the composition is 60% of Co metal, 20% of  $\text{CoAl}_2\text{O}_4$  and 20% CoO while at 25 °C the composition changes to 45% of Co metal, 45% of  $\text{CoAl}_2\text{O}_4$  and 10% CoO. It is worth mentioning that the  $\text{Co}_3\text{O}_4$  standard did not improve the fitting procedure. After 1 h under SRE at 400 °C we have ~33% of reduced Co (metal) and at 500 °C it changes to ~46%, showing structural changes as a function of the temperature of SRE. The final sample at 25 °C after removing the ethanol and water feed (Fig. 1) has ~45% of metallic Co; beside this, the final sample and the sample under SRE do not present an intense pre-edge which indicate the stability of Co symmetry and no more Td sites are formed. The concentration of Co (Td) is stabilized at about 30% under SRE and after the reaction.

We found many reports in the literature [27] showing that the  $\text{CoAl}_2\text{O}_4$  compound is not favorable to catalytic processes because it removes the active phase (Co) from the surface to form this stable phase, spinel, which is inactive or very few active in SRE. But in our sample, after heating at 800 °C in  $\text{H}_2$  atmosphere we estimated by linear combination fit that the sample is formed by 60% of reduced cobalt ( $\text{Co}^\circ$ ) and no  $\text{Co}_3\text{O}_4$  was detected; then decreasing the temperature to 25 °C under He after reduction we achieve ~45% of reduced Co. This variation of reduction state indicates that the Co structure is strongly affected by temperature even under  $\text{H}_2$  or an inert atmosphere, and the  $\text{CoAl}_2\text{O}_4$  phase is not a cumber to reduce the Co in this case.

### 3.1.2. XANES study at Ce $L_{\text{III}}$ -edge

The XANES data from Ce  $L_{\text{III}}$ -edge is frequently used to characterize the electronic properties of ceria-based materials. The spectrum of  $\text{Ce}^{4+}$  presents two intense features in XANES region [28] while one intense feature in the white line is the main characteristic of  $\text{Ce}^{3+}$  spectrum (Fig. 3, up). Fig. 3 (down) shows the XANES of Ce  $L_{\text{III}}$ -edge of fresh sample, reduced sample, under SRE reaction and after the reaction. The characteristic spectrum of  $\text{Ce}^{4+}$  was obtained from our fresh sample. After the reduction, the XANES Ce  $L_{\text{III}}$ -edge presents a typical intense white line of  $\text{Ce}^{3+}$  oxidation state. As the data were collected in transmission mode, we observed that all ceria was reduced from  $\text{CeO}_2 \rightarrow \text{Ce}_2\text{O}_3$  by this activation process. Fig. 4 (up) shows the relative composition of Ce ions along the reduction under  $\text{H}_2$ , obtained by linear combination fit of spectra in Fig. 4 (down) with standards of  $\text{Ce}^{3+}$  and  $\text{Ce}^{4+}$ . Significant changes in Ce spectra were observed at ~580 °C; we achieve 50% of Ce reduction at ~700 °C and the full reduction at 800 °C. After reduction, at 25 °C, we observed a very small decrease in the white line intensity, a small increase in the feature at ~5737 eV and a small energy shift (~0.5 eV), which can indicate that some small content of  $\text{Ce}^{4+}$  can be present in low temperatures even under  $\text{H}_2$ . When the sample is under SRE at 400 °C, 500 °C or under He at 25 °C after reaction, no more significant changes in the Ce  $L_{\text{III}}$ -edge were observed. The mixed oxidation state of Ce ( $\text{Ce}^{3+}$  and  $\text{Ce}^{4+}$ ) was stable in this sample under SRE reaction conditions.

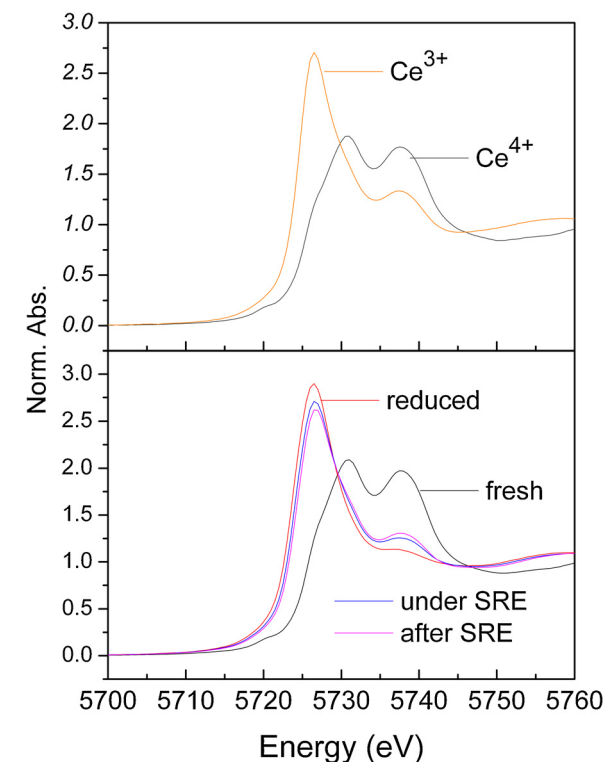


**Fig. 3.** (top)  $\text{CeO}_2$  and  $\text{Ce}(\text{OH})\text{CO}_3$  references of  $\text{Ce}^{4+}$  and  $\text{Ce}^{3+}$  respectively; (bottom) XANES at Ce  $L_{\text{III}}$ -edge from Co5Ce10Al sample under different conditions along the activation and SRE reaction.

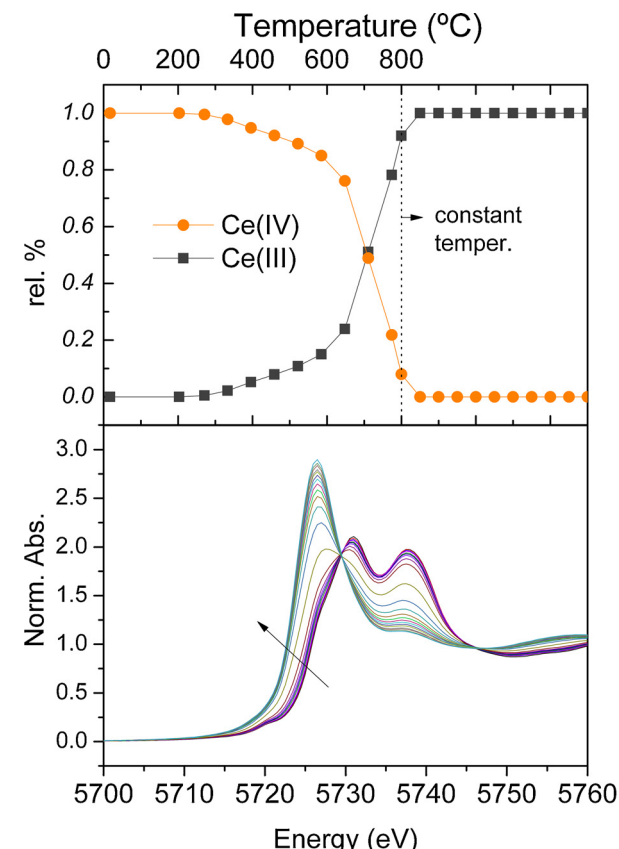


**Fig. 4.** (top) Relative Ce(IV) and Ce(III) fractions in the Co5Ce10Al sample as a function of reduction temperature extracted from the XANES spectra reported in the bottom part; (bottom) evolution of the Ce  $L_{\text{III}}$ -edge XANES of Co5Ce10Al along the reduction process.

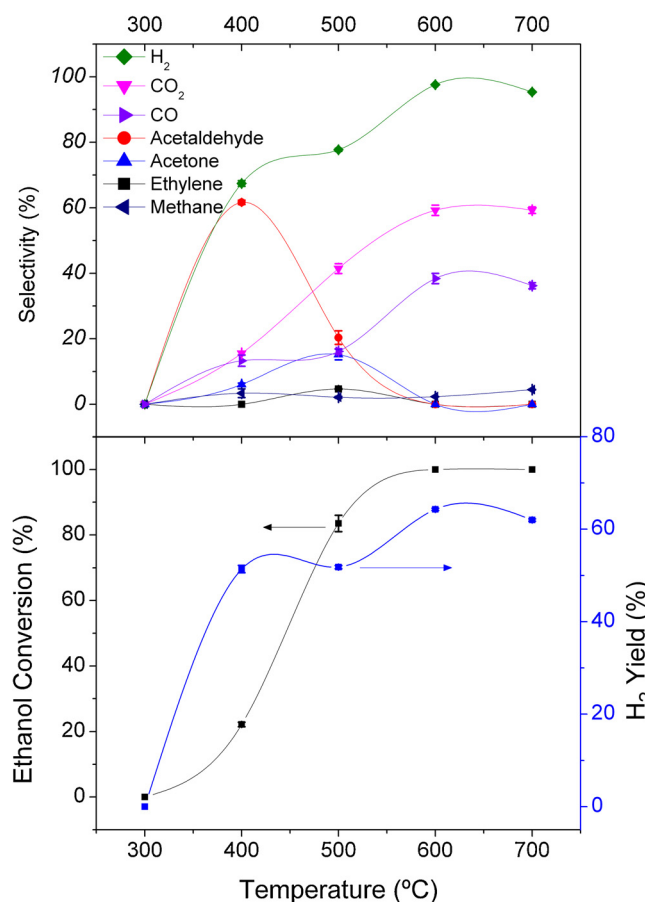


**Fig. 5.** (top) Variation of selectivity to hydrogen, CO<sub>2</sub>, CO, CH<sub>4</sub>, ethylene, acetone, acetaldehyde as a function of temperature; (bottom) Ethanol conversion and hydrogen yield during SRE reaction performed with Co5Ce10Al catalyst.

In Co-alumina supported catalysts, the Co in Td symmetry is a signature of the CoAl<sub>2</sub>O<sub>4</sub>, where Co atoms are not available as active site to catalysis. In Co5Ce10Al sample we aimed to remove all the Co atoms from this structure by adding ceria to our catalyst. By XANES analysis in the Co K-edge and Ce L<sub>III</sub>-edge, the activation process and the presence of Ce in the support seemed to be enough to remove most of Co from this site; later, there was no migration of Co to Td site again by changing to different atmospheres and temperatures. The Ce can be the responsible to remove the Co from the stable structure of CoAl<sub>2</sub>O<sub>4</sub> and then to keep them in Oh symmetry, being irreversible in the tested conditions.

### 3.2. Catalytic reaction

During XANES measurements, the hydrogen production was detected by mass spectrometry (MS) at the tested temperatures (400 and 500 °C). In order to analyze quantitatively the ethanol conversion and hydrogen production, we used Gas Chromatography (GC) to perform catalytic tests with the Co5Ce10Al sample. We attributed the catalytic activity and the structural changes after activation to the Ce presence, which can decrease the thermal stability of CoAl<sub>2</sub>O<sub>4</sub> and favored the atomic diffusion of Co in the catalyst, under temperature and H<sub>2</sub> flux.

All the products evaluated by GC are showed in Fig. 5. The quantitative analysis showed a significant ethanol conversion only at 400 °C and the dehydrogenation of ethanol to acetaldehyde can be observed at this temperature. The higher hydrogen production is also observed at 400 °C. At 500 °C the ethanol conversion drastically increases, and we observe the decreasing on acetaldehyde yield

with the increasing on CO<sub>2</sub> concentration, evidencing the water-gas shift reaction. From 600 °C to 700 °C we observed an increasing on CO concentration, which is expected since the shift reaction is not favored at higher temperatures. The highest amount of methane was only 5% at 700 °C and the ethylene was detected only in 500 °C in concentrations lower than 5%.

This catalyst presented a low selectivity to ethylene, which is one of the main routes for coke formation (the polymerization of ethylene derived from ethanol dehydration) [29]. The coke can cover the active sites decreasing the catalytic conversion. In this case, the Ce can be the responsible to avoid carbon deposits because one of the important properties of cerium oxide is its oxygen storage capacity, which can provide oxygen to the gas mixture in catalytic tests or oxygen mobility over the catalyst surface [30], removing the carbon over the active phase.

During SRE, many authors reported acidic supports like Al<sub>2</sub>O<sub>3</sub> favor dehydration and thereby increase the tendency for coke formation due to the polymerization of ethylene [31]. However, on considered being a basic support as ceria the dehydration is limited and its redox properties inhibit coke formation [32].

Biswas et al. [33] found that a high value of Ce/Zr ratio in Ni-ceria-zirconia catalyst for SRE has a lower tendency for coke formation. Many authors also reported CeO<sub>2</sub>-rich formulations to allow high hydrogen yield [34]. Indeed, the absence of ethylene formation can be the main reason for the low coke formation of our cobalt-ceria-alumina catalysts, even with low ceria content (~10%) as we showed. The oxygen exchange capacity of cerium oxide is associated with its ability to reversibly change the cerium oxidation states between Ce<sup>4+</sup> and Ce<sup>3+</sup> [35]. This mixed oxidation state was detected in XANES Ce L<sub>III</sub>-edge spectra after the reduction at 25 °C and also along all SRE catalytic test, where the ethylene was detected only in very low concentration.

The GC results also showed a low formation of methane, which indicate the undesired reactions that can decrease the hydrogen production (as decomposition of ethanol and acetaldehyde and methanation of CO and CO<sub>2</sub>) are not favored with this catalyst.

On the basis of the above *in situ* and *operando* XANES studies and the catalytic test results, it is possible to propose a reliable structural model, as shown in Fig. 6. The initial state of cobalt species in the sample before reduction exists as CoAl<sub>2</sub>O<sub>4</sub> while the ceria is in CeO<sub>2</sub> form (Ce<sup>4+</sup>). The reduction transforms aluminate to cobalt oxide (CoO) and metal clusters (Co); the ceria is fully reduced from Ce<sup>4+</sup> to Ce<sup>3+</sup>; the cobalt species attaches on the surface of ceria (now Ce<sub>2</sub>O<sub>3</sub> in high temperatures). It is, therefore, concluded that the cobalt species are dispersed on the ceria surface, interacting with ceria in the Co5Ce10Al catalyst. During SRE up to the end of reaction, the Co/CoO ratio increase with the increase of temperature and the Co concentration in CoAl<sub>2</sub>O<sub>4</sub> site is kept constant; a small amount of Ce<sup>4+</sup> is formed; the mixture of Ce<sup>4+</sup>/Ce<sup>3+</sup> is stable and no CoAl<sub>2</sub>O<sub>4</sub> formation is detected.

### 4. Conclusions

We studied the influence of Ce on Co/CeO<sub>2</sub>/Al<sub>2</sub>O<sub>3</sub> catalyst. The Ce presence contributed to activate the catalyst and even with the presence of CoAl<sub>2</sub>O<sub>4</sub> we obtained a sample with a mixture of compounds which presented high hydrogen selectivity by SRE reaction. The interaction between Co and Ce showed a significant improvement in the reducibility of Co and an important role to avoid the formation of CoAl<sub>2</sub>O<sub>4</sub> again.

The catalyst evaluation showed high ethanol conversion followed by high hydrogen yield at 500 °C. The products analysis at this temperature showed a reaction pathway through the acetaldehyde route. The CO<sub>2</sub> selectivity showed a water-gas shift reaction consuming CO to produce hydrogen. The methane formation was

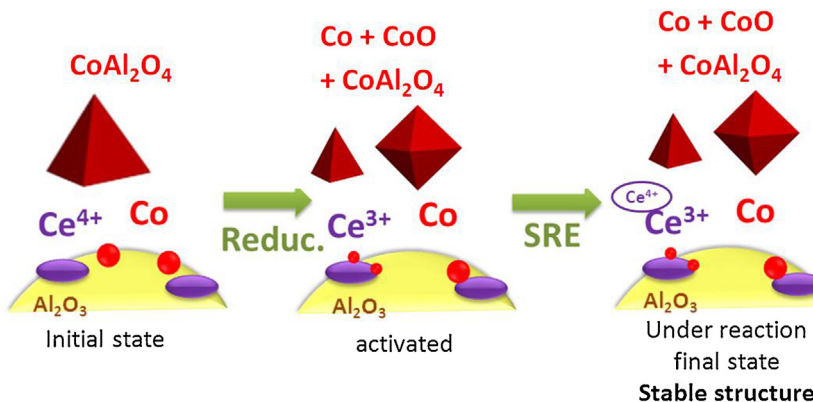


**Fig. 6.** Structural model proposed to the Co5Ce10Al catalyst in different steps of reaction. The initial state shows the presence of  $\text{CoAl}_2\text{O}_4$  compound; the activation step shows the reduction of  $\text{Ce}^{4+}$  to  $\text{Ce}^{3+}$  and the structural change in the Co site; the final structure shows a small oxidation of Ceria and Co predominant in Oh site.

below 4.5% in all tested temperatures. The methane presence can be an issue to decrease the hydrogen production since the methane reforming reaction requires higher temperatures. The ethylene can be a source to carbon formation over the active sites, but this catalyst also presented a low selectivity to ethylene.

## Acknowledgements

We thank Dr. Daniela Zanchet and Felipe Moreira Pinto for the GC analysis. We also thank the financial support from FAPESP (proc. 2013/18062-2 and 2014/2666-1) and the Brazilian Synchrotron Light Laboratory (LNLS) at CNPEM for the use of XAFS1 beamline installation (internal proc.). Narciso Souza-Neto is acknowledged for the manuscript revision.

## References

- [1] V.A. Goltssov, T.N. Veziroglu, L.F. Goltsova, Int. J. Hydrogen Energy 31 (2) (2006) 153–159.
- [2] E. Seker, Int. J. Hydrogen Energy 33 (2008) 2044–2052.
- [3] C. Graschinsky, M. Laborde, N. Amadeo, A. Le Valant, N. Bion, F. Epron, D. Duprez, Ind. Eng. Chem. Res. 49 (24) (2010) 12383–12389.
- [4] J.P. Breen, R. Burch, H.M. Coleman, Appl. Catal. B: Environ. 39 (1) (2002) 65–74.
- [5] M. Ni, D.Y.C. Leung, M.K.H. Leung, Int. J. Hydrogen Energy 32 (15) (2007) 3238–3247.
- [6] T. Apichai, S. Tawee, T. Supaporn, Sci. Asia 27 (2001) 193–198.
- [7] F. Haga, T. Nakajima, H.M.S. Mishima, Catal. Lett. 48 (1997) 223–227.
- [8] J. Llorca, N. Homs, J. Sales, P.R. de la Piscina, J. Catal. 209 (2002) 306–317.
- [9] M. Benito, J.L. Sanz, R. Isabel, R. Padilla, R. Arjona, L. Daza, J. Power Sources 151 (0) (2005) 11–17.
- [10] H. Wang, Y. Liu, L. Wang, Y.N. Qin, Chem. Eng. J. 145 (2008) 25–31.
- [11] C. Resini, T. Montanari, L. Barattini, G. Ramis, G. Busca, S. Presto, P. Riani, R. Marazza, M. Sisani, F. Marmottini, U. Costantino, Appl. Catal. A: Gen. 355 (2009) 83–93.
- [12] J.L. Contreras, J. Salmones, J.A. Colín-Luna, L. Nuno, B. Quintana, I. Cordoba, B. Zeifert, C. Tapia, G.A. Fuentes, Int. J. Hydrogen Energy 39 (2014) 18835–18853.
- [13] J. Llorca, N. Holms, P.R. de la Piscina, J. Catal. 227 (2004) 556–560.
- [14] J. Llorca, P.R. de la Piscina, J.A. Dalmon, J. Sales, N. Holms, Appl. Catal. B: Environ. 43 (2003) 355–369.
- [15] I.I. Soylak, H. Sohn, U.S. Ozkan, ACS Catal. 2 (2012) 2335–2348.
- [16] A. Erdohelyi, J. Raskó, T. Kecskés, M. Tóth, M. Dömök, K. Baán, Catal. Today 116 (2006) 367–376.
- [17] G. Busca, U. Costantino, T. Montanari, G. Ramis, C. Resini, M. Sisani, Int. J. Hydrogen Energy 35 (2010) 5356–5366.
- [18] H. Song, U.S. Ozkan, J. Catal. 261 (2009) 66–74.
- [19] E. Varga, Z. Ferencz, A. Oszkó, A. Erdohelyi, J. Kiss, J. Mol. Catal. A: Chem. 397 (2015) 127–133.
- [20] A.J. Frenkel, J.A. Rodriguez, J.G. Chen, ACS Catal. 2 (2012) 2269–2280.
- [21] M. Fernandez-Garcia, Catal. Rev. Sci. Eng. 44 (2002) 59–121.
- [22] S. Bordiga, E. Groppo, G. Agostini, J.A. van Bokhoven, C. Lamberti, Chem. Rev. 113 (2013) 1736–1850.
- [23] M.A. Newton, A.J. Dent, J. Evans, Chem. Soc. Rev. 31 (2002) 83–95.
- [24] F. Frusteri, S. Freni, V. Chiodo, S. Donato, G. Bonura, S. Cavallaro, Int. J. Hydrogen Energy 31 (2006) 2193–2199.
- [25] E.C. Wanat, K. Venkataraman, L.D. Schmidt, Appl. Cat. A: Gen. 276 (2004) 155–162.
- [26] H.Y. Jeong, D.-C. Koh, K.-S. Lee, H.H. Lee, Appl. Catal. B: Environ. 127 (2012) 68–76.
- [27] S.D. Davidson, H. Zhang, J. Sun, Y. Wang, Dalton Trans. 43 (2014) 11782–11802.
- [28] X. Wang, J.A. Rodriguez, J.C. Hanson, D. Gamarra, A. Martínez-Arias, M. Fernández-García, Top. Catal. 49 (2008) 81–88.
- [29] D. Li, L. Zeng, X. Li, X. Wang, H. Ma, S. Assabumrungrat, J. Gong, Appl. Catal. B: Environ. 176–177 (2015) 532–541.
- [30] D. Zanchet, J.B.O. Santos, S. Damyanova, J.M.R. Gallo, J.M.C. Bueno, ACS Catal. 5 (2015) 3841–3863.
- [31] M. Badlani, I.E. Wachs, Catal. Lett. 75 (2001) 137–149.
- [32] L.V. Mattos, B.H. Jacobs, F.B. Noronha, Chem. Rev. 112 (2012) 4094–4123.
- [33] P. Biswas, D. Kunzru, Int. J. Hydrogen Energy 32 (2007) 969–980.
- [34] M. Liao, W. Wang, R. Ran, Z. Shao, J. Power Sources 196 (2011) 6177–6185.
- [35] J. Kaspar, P. Fornasiero, M. Graziani, Catal. Today 50 (1999) 285–298.